Geotechnical Analysis of Pile-Supported Embankments on Soft Soils

Suresh Kommu[1*], and *Raikanti* Amulya[1]
[1]Department of Civil Engineering, VNR Vignana Jyothi Institute of Engineering and Technology, Hyderabad, India.

Abstract. Construction on soft soils often results in significant settlement and other structural failures. In the case of very soft soils that are unsuitable for direct construction, a piled embankment provides a stable and reliable platform. When designing the piled embankment, there are two relevant factors, both related to the geosynthetic material of the geogrid, which include its stiffness and placement at the base of the embankment. In the present study, the embankment is constructed over soft soils such as peat, clay, and sand. Geosynthetic reinforcement, specifically geogrids, is used to enhance embankment performance. This piled embankment is the best solution that reduces large settlement and economically constructs the geosynthetic materials that are used as reinforcement to increase platform stability. A finite element analysis, PLAXIS 2D, is performed to calculate the tensile force acting on the geogrid and resulting settlements at a range of stiffness from 300 kN/m to 30000 kN/m. It is seen that as the geogrid's stiffness increases, the tensile force increases and therefore causes settlement to decrease. Finally, Terzaghi's trapdoor test is used to develop theoretical formulae for calculating stresses induced by the arching effect in embankments.

1 Introduction

Pile-supported embankments are becoming more popular as an eco-friendly infrastructure option because they enable quicker construction on unstable subsoils like peat and marine clay. In this context, vertical piles, transfer platforms, and basal geosynthetics have recently been incorporated into ground improvement methods to prevent adverse long-term effects, reduce differential settlements, and overall enhance the strength of embankments [1]. The current work combines sophisticated numerical modeling with theoretical evaluation based on performance-based geotechnical design concepts [2]. Quantifying settlement reduction, comprehending soil-pile interaction, and investigating the impact of geogrid stiffness on the soil arching process under static loading circumstances are the main objectives.

* Corresponding author: suresh_k@vnrvjiet.in

The piled embankment is to create a strong platform on top of the soft soil, which has large deformations, so that soils are supported by the pile and able to construct an embankment within a short period with reduced settlement and failures. Most of the time, piled embankments are utilized to limit residual settlement after construction and are placed near bridges or hard shoulders. When no settlement exists, the transition zone will be improved because of this, when the building duration prevents the use of standard consolidation [3]

The usage of the piled embankment is one of the most potential solutions for this issue. This method looks to be the most feasible, efficient, and environmentally friendly method for building on soft soil in many circumstances [4, 5]. Highways, railways, and the development of fill areas for industrial or residential purposes are the most common field applications [6, 7].

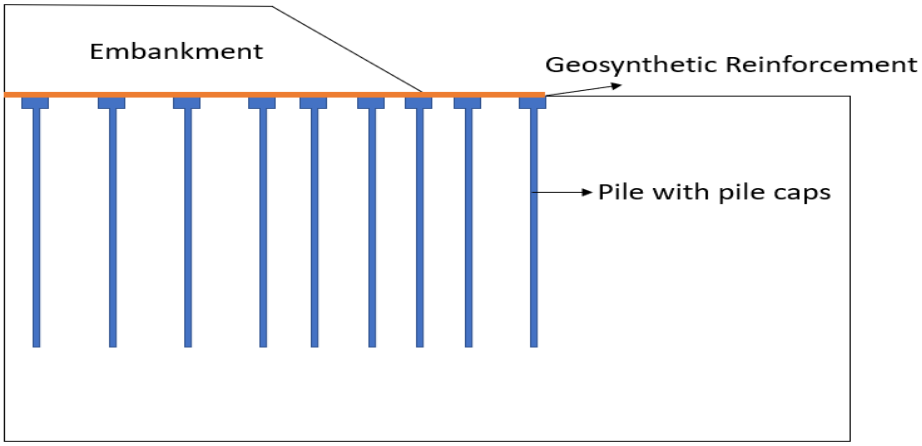

Fig.1. Geosynthetic Reinforced Piled Embankment

The height of the fill and the pile material's elastic modulus were affected by the geosynthetic tensile stiffness . Tensile stiffness becomes less significant at 4000 kN/m. The pile's elastic modulus is 30,000 MPa. Because the tensile strain is not constant along the length of the reinforcement, maximum tension occurs near the edge of the pile, and maximum settlement is reduced by up to 20%, reinforced pile embankments perform better than unreinforced pile embankments [8, 9]. In PLAXIS 2D, the numerical modelling uses the geogrid as the separation material to allow the geotextile and fill material to lessen the settlement [10]. The earlier research factored in the subsoil's condition, which is organic clay with high plasticity and moisture, while the upper layer is mangrove with roots. Additionally, it was observed that the crack propagation to the crown has the fastest rate of propagation towards the fill's toe.

The embankment measured 120 m long and 5.6 m wide with a 1V:1.5H slope, having a crowned width of 35 m. To measure the earth pressure surrounding the pile, pressure cells were erected, settlement plates were placed on the surrounding soil, and a piezometer was placed at the center of the embankment. Approximately 14 times more pressure was applied to the pile head than to the surrounding soil. When the piled embankment was being built, the measured lateral displacement-settlement ratio was roughly 0.2. The behavior of piled supported approach embankments with transfer layers by analytical and numerical methods. The observational approach is then used to evaluate PVD performance and settlement estimates, with a focus on minimizing residual settlements. The soil is made up of coastal

clay. The results of numerical evaluations of Geosynthetic-Reinforced Pile-Supported (GRPS) embankments employed in approaches close to structures using PLAXIS software. Using slope stability analysis with Geo Studio, the factor of safety was found to be 1.83 under design parameters of 10 kN/m^2 of construction loading and 20 kN/m^2, 0% surcharge load, and embankment height of 2.5 m of soft clay soils. A full-scale field test of GRPESs served as the basis for calibrating the numerical models employed in this investigation. The maximum tensile force produced internally in the geosynthetic reinforcement and the load distributions absorbed by the various components of the numerical models simulating GRPESs were compared with comparative analysis, design approach analysis, and other analytical results when comparing the models [11]. The same stiffness value (1180 kN/m) was used to numerically assess the stiffness of single and multilayer layers. The bearing capacity of a single pile was evaluated using two standards: the AASHTO-LRFD Bridge Design Specifications and the Chinese National Standard (CNS, 2002). The projected bearing capacity was compared with the FEM analysis based on GB 50007–2002. Young's modulus of 28 and 30 GPa, Poisson's ratio of 0.15 and 0.10, and unit weight of 24 and 26 kN/m³ are among the pile cap characteristics taken into consideration. The model was subjected to a load of 445 kPa, and PLAXIS 3D was used to do a numerical analysis of the pile parameters. The AASHTO code's allowable limits are met with the maximum displacement of –20.95 mm.

However, the pile bearing capacity determined by the AASHTO code is only 65.57 percent of that determined by the Chinese code. The AASHTO code is more adjustable than the Chinese regulations for shear design. Soil arching can be defined as the concentration of stresses around the pile due to the stiffness difference between the soft foundation soil and the rigid pile [12].

The findings demonstrate a robust correlation between the geogrid's stiffness and settlement mitigation efficacy. For stiffness larger than 15,000 kN/m, the settlement drop reaches 50%, with declining returns beyond this. The stress concentration ratio (SCR) under optimal conditions was 4.2, which is in line with empirical predictions.

2 Methodology

2.1 Numerical simulation

The foundation soils, piling, and embankment fill were represented in a PLAXIS 2D finite element model as 15-node triangular elements simulating the coupled phenomena. Border reflection was eliminated through expanding the model boundaries laterally to 60 m and 25 m in depth. Additionally, interface elements were assigned between the piles and the surrounding soil based on strength reduction factors to capture potential partial slide conditions.

By utilizing a staged building approach, it was possible to observe stress redistribution at each density level by modelling filling in 0.6 m lifts. The geogrid layer was modelled as an elastic element possessing variable stiffness. The numerical model incorporated both instantaneous elastic settlement and subsequent consolidation effects which were calibrated using laboratory permeability data obtained for both clay and peat.

In the present study, the numerical simulation of the piled embankment is done by using PLAXIS 2D. Both the piles and the top of the pile consist of cylindrical shapes. As there will be some friction between the soft soil (foundation soil) and rigid piles, and considering that the soil will be disturbed more than pile height, we will consider an interface approach defined on both sides of the pile with an additional 0.5m at the bottom. The typical spacing

between piles is recommended as a minimum of 1.5 to 4.5m. In this study, a 3m center-to-center spacing was used based on the literature. The piles are modelled as a non-porous material with a unit weight of (25 kg/m^3), and the diameter of the pile is (0.3m), and the pile cap (0.5 m). In this study, a surcharge of 24 kpa was applied, as specified in (IRC: 75:2015).

A layer of peat soil measuring six meters is present above the sand and clay. In this case, a layer of 25 meters of foundation soil geosynthetic material is utilized as the tension member. A tension member symbolizes the usage of a single layer of geosynthetic; when multiple layers are utilized, that's referred to as the loading platform. Because there are four types of materials - pile, embankment fill, foundation soil, and geosynthetic material - the design of piled embankments is a contentious issue. The last numerical analysis was applied to resolve this problem. An analysis, particularly representing geosynthetic material as the elastoplastic material, utilizes a stiffness range of 300 kN/m to 30000 kN/m to represent the pile as the non-porous material representing the embankment fill in staged construction, each of which has a rise of 0.6m. We shall continue to note the geosynthetic material. The best geosynthetic material for piled embankments on soft soil is geogrid, and overall, the selected model type is axisymmetric and has 15 nodes. The model's boundary conditions allow for both fixed displacement at the bottom and free displacement at the sides. The finished PLAXIS 2D model is displayed in Figure 2. The soil–pile interface is the contact zone between the pile surface and the surrounding soil, where load transfer and interaction occur.

Table 1. The material properties of the study

Type of soil	**Unit weight of soil (kN/m^3)**	**Elasticity Modulus (kN/m^2)**	**Cohesión (c) (kN/m^2)**	**Friction angle**	**Poisson's ratio**
Embankment soil	20	25000	1	30	0.3
Peat	8	5000	2	23	0.45
Clay	16	5000	5	0	0.49
Sand	17	50000	0	33	0.3
Pile	24	30*10^6			0.15
Pile cap	24	30*10^6			0.15

For the peat, the project used stiffness parameters of λ=0.15 and k*=0.03. [13]

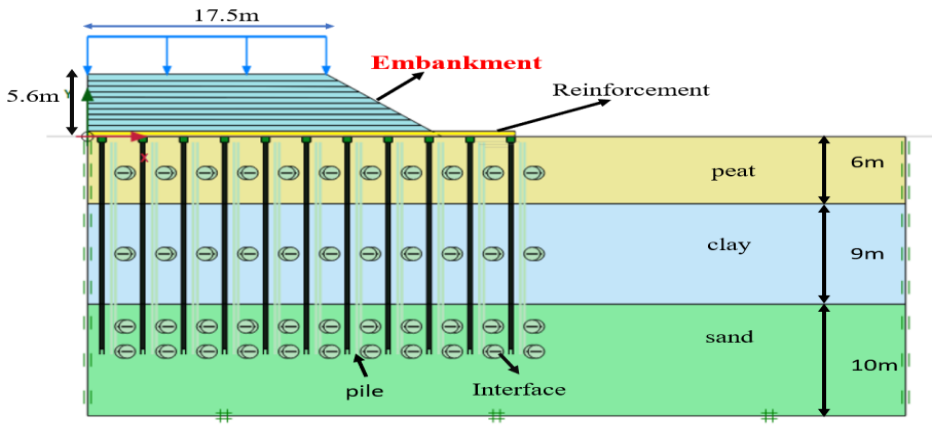

Fig.2. Numerical model for the analysis

2.2 Soil arching causes vertical stress: Theoretical Solution

The load on the pile divided by the load on the surrounding ground is known as the arching ratio, and it falls as the embankment's height rises. The stress contribution from the arching is determined with the help of formulae derived from Terzaghi's trap door test. The theoretical analyses presented by Hewlett and Randolph, along with the British Standard BS 8006 (1995), do not account for the effects of geosynthetic or pile stiffness, as discussed by Eekelen et al. [14] in their study titled Analysis and Modification of the British Standard BS8006 for the Design of Piled Embankments. However, the present methodology captures the properties of the reinforcing material.

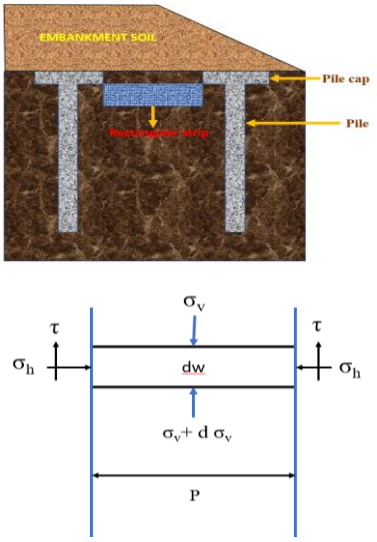

Fig.3. Analytical model for deriving the formulae for the vertical stress

Based on the Terzaghi trapdoor test, Forces acting on the rectangular strip, Weight of the strip (dw) = ϒ*A*dz, ϒ = unit weight of the strip (kN/m^3); A= width of the rectangular strip (m), dz= thickness of the rectangular strip, Shear stress (τ) = c+ σ_h tanδ, σ_h = lateral earth pressure of reinforced zone (kN/m^2); σ_h= σ_v k, σ_v = vertical stress of the reinforced zone.

Shear load (ds) = c+ σ_h tanδ and assuming granular soil c = 0, the following equation can be derived to calculate the vertical stress.

Equilibrium of forces: Sum of upward forces = downward forces

$$\tau + \sigma_v + d\sigma_v = dw + \sigma v \quad (1)$$

$$\sigma_v * p + \Upsilon * p * dz = (\sigma_v + d\sigma_v) * p + (\sigma_v k \tan \delta)\, dz$$

$$\Upsilon * p * dz = d\sigma_v * p + \sigma_v k \tan\delta\, dz$$

Dividing the equation by the area of the strip

$$\frac{\Upsilon * p * dz}{p * dz} = \frac{d * \sigma v * p}{p * dz} + \frac{\sigma v * k * \tan\delta}{p * dz} * dz$$

$$Let\ x = \Upsilon;\ y = \frac{k \tan\delta}{p}$$

$$\frac{d\,\sigma v}{dz} = x\text{-}y\ \sigma_v \quad (2)$$

Integrating on both sides

$$\int_0^{\sigma v} \frac{d\,\sigma v}{X - Y\,\sigma v} = \int_0^{z} dz$$

$$\left[\frac{-1}{Y}\ln(X - Y\sigma_v)\right]_0^{\sigma_v} = [z]_0^z$$

$$\frac{\ln(X - Y\sigma v)}{\ln(X)} = -Yz$$

$$\frac{X - Y\sigma v}{X} = e^{-Yz}$$

$$\frac{X(1 - e^{-Yz})}{Y} = \sigma_v$$

$$\sigma_v = \frac{Y\left(e^{\frac{-k\tan\delta}{p}z}\right)}{\frac{k\tan\delta}{p}} \quad (3)$$

Equation (3) is a calculation for vertical stress acting due to arching, where p is the length of the strip, k is the constant, and δ is the internal friction angle.

3 Results and discussion

3.1 Settlement at the foundation (Displacement analysis)

Peat is the weakest of all soft soils; there will be substantial settlements. Differential settlement occurs when the amount of settlement at the pile head is smaller than the amount of settlement at a higher elevation between the piles. Patrons are offered in order to reduce the number of settlements along the embankment's base. Deformation was decreased by up to 18% for 3000 kN/m, 28% for 16500 kN/m, and 48% to 49% for 30000 kN/m, respectively, by making the reinforcement more rigid. The effects of the geogrid decreased as the plaza reinforcement's rigidity was increased to 16500kN/m. The settlements shown in Figure 4 are at the surface of the gene again; to eliminate settlements, the base needs to be reinforced with resistance and increased stiffness. The settlement is relatively small by the approximate outcome of this smaller soil padding; however, as the stiffness of the resistance increased, hence increased the rigidity of the soft soil also increased, then it would see significantly less development of soil arching.

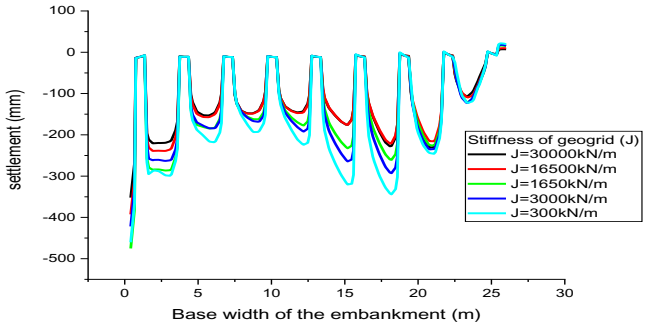

Fig.4. Graph for the settlements for the different stiffness

3.2 Maximum tensile force

The tensile force has grown as the geogrid's stiffness has increased, and these findings are consistent with those of Tuan A. Pham [12]. The tensile force is not uniform throughout the length of the reinforcement, as shown in the Figure 5. When compared to the pile cap's edges and between them, the middle of the pile cap experiences the highest tension. Tensile

force diminishes as the soft soil modulus becomes more rigid. Figure 5 clearly illustrates the tensile force throughout the embankment's breadth for varying geogrid stiffnesses between 300 kN/m and 30,000 kN/m. The reinforcement's tensile force progressively rises from 300kN/m to 3000kN/m. tensile force increases by up to 44% and 57% for the 16500 kN/m and 30000 kN/m, respectively, depending on the geogrid's stiffness.

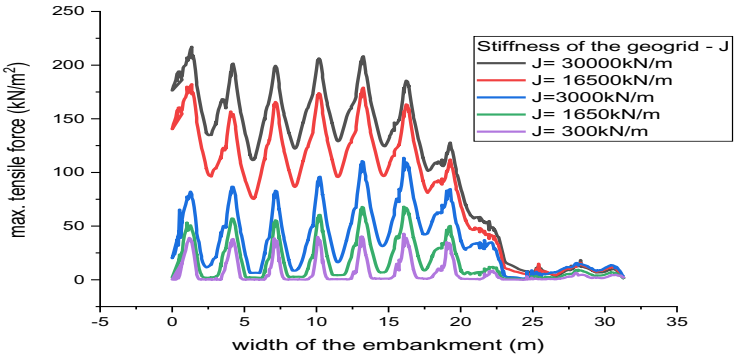

Fig.5. Graph of tensile force in the reinforcement for various stiffness

3.3 Vertical stress

For the vertical stress in PLAXIS 2D Cartesian effective stress is observed. From the numerical modelling, the result obtained as the piles carry the greatest vertical stress. When compared to edge piles, centre piles take on the most vertical stress (lateral piles). The distribution of stress is shown in Figure 6.

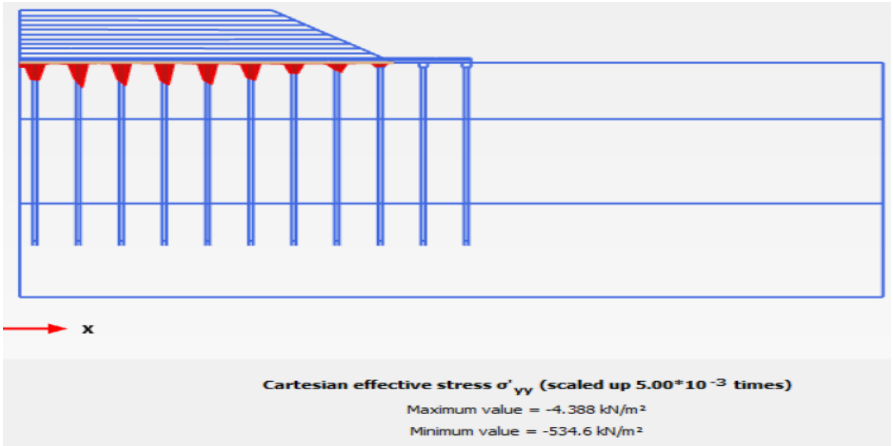

Fig.6. Vertical stress distribution at the base of the embankment

The stress taken by the piles is 80% more than the stress taken by the soil, and as the stiffness of the geogrid increases, the stress taken by the soil increases. The graph shown for the vertical stress for the different stiffnesses of geogrid is shown in Figure 7.

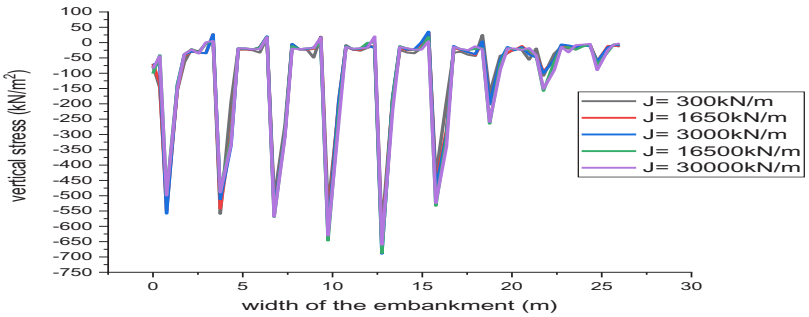

Fig.7. Vertical stress distribution for the different stiffnesses of the geogrid

3.4 Bending moment of piles

In a geosynthetic reinforced piled embankment, large lateral piles are avoided because, unlike Raking Piles, the reinforcement material does an acceptable job of resisting the lateral thrust with no required raking piles. Because of the structure's symmetry, the bending moments that happen at the end piles are greater (It was not focusing on pile number 1). Additionally, the bending moments of the piles at the embankment's toe are increased by lateral stresses. Lastly, Figure 8 displays the piles' bending moments as a result of the numerical modelling. In considering the bending moment of piles, structural forces are calculated as shown in Figure 9. The expanding section at the piles shows how far the pile is bending or has engaged the bending moment action.

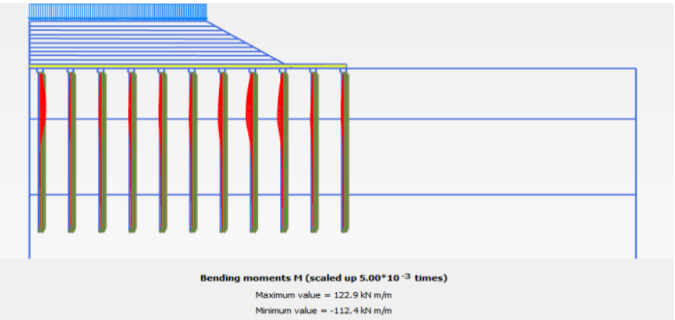

Fig.8. Output from the PLAXIS 2D for the bending moment of piles

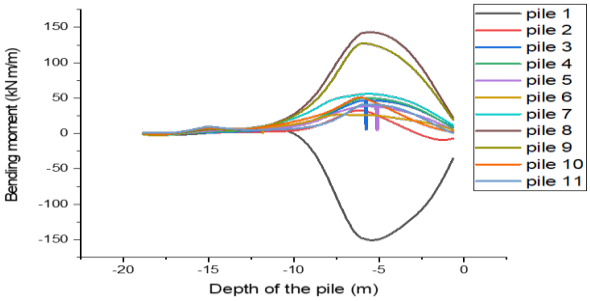

Fig.9. Graph for the bending moment of each pile

4 Conclusions

The following conclusions were drawn from the analysis. The major key findings and concluding points are presented below.

- As the stiffness of the geogrid grows from 300 kN/m to 30000 kN/m, the biggest settlements are observed at 16500 kN/m. After 16500 kN/m, any increase is insignificant; thus, 16500 kN/m is the ideal stiffness range between 300 kN/m and 30000 kN/m.
- The settlements due to this stiffness produce the lowest values noted.
- The shear stress in the foundation soil is reduced as the reinforcement tensile strength is improved.
- The tensile resistance of the reinforcement is improved by 44%.
- The shear stress in the foundation soil is lowered by 2.34 percent.
- The arching effect from the basis of the reinforced structure is due to the stiffness difference between the installation and the adjacent soil.

5 Future scope

This study worked on a single layer of the reinforcement, so further analysis can be done for the multiple layers of reinforcement.

References

1. Minh-Tuan Pham, Duc-Dung Pham, Duy-Liem Vu and Daniel Dias, Embankments Reinforced by Vertical Inclusions on Soft Soil: Numerical Study of Stress Redistribution, *Geotechnics*, ***3***(4),(2023). https://doi.org/10.3390/geotechnics3040069
2. Wei-Kang Lin, Bin Mao, Bing Duan, Numerical Analysis of Pile-Supported Reinforced Embankments in Deep Soft Soil Regions Based on Soft Soil Creep Parameter Optimization, Adv.CE, (2025). https://doi.org/10.1155/adce/1759641
3. Pengyu Li, Hongqiang Dou, Hao Wang, , Wen-Feng Nie and Fu-Quan Chen**,** Stability Analysis of Pile-Supported Embankments over Soft Clay Considering Soil Failure between Piles Based on Upper Bound Theorem**,** Sustainability, Vol.**14** , Issue 18 , (2022). https://doi.org/10.3390/su141811652
4. Yuvraj , Sunita Kumari, Embankment Resting on Problematic Soil: A Critical Review, SSRG IJCE, Vol. **11** Issue 12, 69-80, (2024). https://doi.org/10.14445/23488352/IJCE-V11I12P107
5. Mohamed A. Sakr, Waseim R. Azzam and Mohamed A. Sallam, Performance of Pile Supported Embankments over Soft Clay, ASGE Vol. **03** (02), pp. 14-25, (2022). DOI: 10.21608/asge.2022.152711.1010
6. S. J. M. van Eekelen;, J. Han, Geosynthetic-reinforced pile-supported embankments, **27 (2),** 112–141,G I (2020). https://doi.org/10.1680/jgein.20.00005
7. Viviana Mangraviti, Luca Flessati, Claudio di Prisco, Geosynthetic-reinforced and pile-supported embankments: theoretical discussion of finite difference numerical analyses results, EJECE,Vol.**27,** Issue 15, Pages 4337-4363,, (2023). https://doi.org/10.1080/19648189.2023.2190400
8. Geye Li , Chao Xu , Chungsik Yoo , Panpan Shen , Qingming Wang , Performance of unreinforced and geogrid-reinforced pile-supported embankments under localized

surface loading: Analytical investigation, GG, Vol.53, Issue 1 , Pages 260-276, (2025). https://doi.org/10.1016/j.geotexmem.2024.09.017

9. Essam Badrawi, Marcela Bindzarova Gergelova, Kamila Kotrasova, and Rana Hassan, Enhancement of the Behavior of the Soft Clay Layer Under the Embankment Using Pu-Foam Pile, *Appl. Sci.* *15*(22), (**2025**). https://doi.org/10.3390/app152212166
10. Rashad Alsirawan, Ammar Alnmr, and Edina Koch, Experimental and Numerical Investigation of Geosynthetic-Reinforced Pile-Supported Embankments for Loose Sandy Soils, *Buildings* , *13*(9), 2179; (**2023). https://doi.org/10.3390/buildings13092179**
11. A. Ikbarieh, Finite element numerical modeling and parametric study of geosynthetic reinforced pile-supported embankments. Louisiana State Univ., PhD Thesis (2022). https://doi.org/10.31390/gradschool_theses.5406
12. Tuan A. Pham, Analysis of geosynthetic-reinforced pile-supported embankment withsoil-structure interaction models, Computers and Geotechnics, Vol.**121,** (2020). https://doi.org/10.1016/j.compgeo.2020.103438
13. B.D. Surya, S. Kommu, Numerical modelling of secant piles**.** IOP Conf. Ser.: Earth Environ. Sci. **1280**(1), 012040 (2023). https://doi.org/10.1088/1755-1315/1280/1/012040
14. S.J.M. van Eekelen, A. Bezuijen, F. van Tol, Analysis and modification of the British Standard BS8006 for the design of piled embankments. Geotext. Geomembr. **29**(3), 345–359 (2011). https://doi.org/10.1016/j.geotexmem.2011.02.001